Modulation of the Estrogen/erbB2 Receptors Cross-talk by CDK4/6 Inhibition Triggers Sustained Senescence in Estrogen Receptor– and ErbB2-positive Breast Cancer

Lucia Viganò[1], Alberta Locatelli[1], Adele Ulisse[1], Barbara Galbardi[1], Matteo Dugo[1], Diego Tosi[2], Carlo Tacchetti[3], Tiziana Daniele[3], Balázs Győrffy[4,5,6], Lorenzo Sica[1], Marina Macchini[1], Milvia Zambetti[1], Stefania Zambelli[1], Giampaolo Bianchini[1], and Luca Gianni[7]

ABSTRACT

Purpose: The interplay between estrogen receptor (ER) and erbB tyrosine-kinase receptors (RTK) impacts growth and progression of ER-positive (ER^+)/HER2-positive ($HER2^+$) breast cancer and generates mitogenic signals converging onto the Cyclin-D1/CDK4/6 complex. We probed this cross-talk combining endocrine-therapy (fulvestrant), dual HER2-blockade (trastuzumab and pertuzumab), and CDK4/6-inhibition (palbociclib; PFHPert).

Experimental Design: Cytotoxic drug effects, interactions, and pharmacodynamics were studied after 72 hours of treatment and over 6 more days of culture after drug wash-out in three $ER^+/HER2^+$, two $HER2^{low}$, and two ER-negative (ER^-)/$HER2^+$ breast cancer cell lines. We assessed gene-expression dynamic and association with Ki67 downregulation in 28 patients with $ER^+/HER2^+$ breast cancer treated with neoadjuvant PFHPert in NA-PHER2 trial (NCT02530424).

Results: *In vitro*, palbociclib and/or fulvestrant induced a functional activation of RTKs signalling. PFHPert had additive or synergistic antiproliferative activity, interfered with resistance mechanisms linked to the RTKs/Akt/MTORC1 axis and induced sustained senescence. Unexpected synergism was found in $HER2^{low}$ cells. In patients, Ki67 downregulation at week 2 and surgery were significantly associated to upregulation of senescence-related genes ($P = 7.7E\text{-}4$ and $P = 1.8E\text{-}4$, respectively). Activation of MTORC1 pathway was associated with high Ki67 at surgery ($P = 0.019$).

Conclusions: Resistance associated with the combination of drugs targeting ER and HER2 can be bypassed by cotargeting Rb, enhancing transition from quiescence to sustained senescence. MTORC1 pathway activation is a potential mechanism of escape and RTKs functional activation may be an alternative pathway for survival also in $ER^+/HER2^{low}$ tumor. PFHPert combination is an effective chemotherapy-free regimen for $ER^+/HER2^+$ breast cancer, and the mechanistic elucidation of sensitivity/resistance patterns may provide insights for further treatment refinement.

Introduction

Breast cancer with estrogen receptor α (ERα) expression [ER-positive (ER^+)] and erbB2 overexpression [IHC 3-positive (3^+) and/or HER2-gene amplified; HER2-positive ($HER2^+$)] has relatively low sensitivity to ER-directed therapies (1, 2). This well-known clinical observation has been attributed to a cross-talk between ER and HER2 so that constitutively increased HER2 signaling can augment ERα function and lead to relative resistance to endocrine therapy (3, 4). Clinical trials showed that the addition of the anti-HER2 drugs trastuzumab (5) or lapatinib (6) to aromatase inhibitors led to only modest improvement of therapeutic results, suggesting that the disruption of the bidirectional cross-talk between HER2 and ERα is bypassed by alternative pathways of tumor survival. Of note, the mitogenic signals driven by tyrosine kinase receptors (RTK) and hormone receptors (HR) converge to the Cyclin-D1/CDK4/6 complex, which is a key regulator of the G1-S transition and cell cycle progression (7–9).

Pharmacologic inhibition of CDK4/6 with small molecules such as palbociclib has relevant therapeutic activity in preclinical models and in human breast cancer (10). Preclinical data demonstrated that HR-positive (HR^+) cell lines were more sensitive than HR-negative (HR^-) to palbociclib (11). This is probably due to HR^+ tumor cells being less frequently Rb-negative (11), and commonly having high levels of cyclin D1 (12) and low expression of the inhibitor p16 (CDKN2A). Benefit from palbociclib and other CDK4/6 inhibitors combined with endocrine therapies was initially reported by Finn and colleagues (11) and confirmed in numerous clinical trials in HR^+/HER2-negative ($HER2^-$) breast cancer (13–18), and the combinations are now a standard of therapy in women with HR^+ metastatic breast cancer.

In vitro HER2 amplified cell lines showed high sensitivity to palbociclib indicating the relevance of cyclin D1-CDK4/6 activity for the initiation and maintenance of HER2-driven breast cancer (10). Of note, the efficacy of the combination of CDK4/6 inhibitors with trastuzumab or lapatinib was more than additive (11, 19).

[1]Department of Medical Oncology, IRCCS San Raffaele Scientific Institute, Milan, Italy. [2]Institut régional du Cancer de Montpellier (ICM), Montpellier, France. [3]Experimental Imaging Centre, IRCCS San Raffaele Scientific Institute, Milan, Italy. [4]Department of Bioinformatics, Faculty of General Medicine, Semmelweis University, Budapest, Hungary. [5]2nd Dept. of Pediatrics, Faculty of Medicine, Semmelweis University, Budapest, Hungary. [6]TTK Oncology Biomarker Research Group, Institute of Enzymology, Budapest, Hungary. [7]Fondazione Michelangelo, Milan, Italy.

L. Viganò and A. Locatelli contributed equally to this article.

Corresponding Authors: Luca Gianni, Fondazione Michelangelo, Via Agostino Bertani, 14, Milan 20121, Italy. Phone: 390-2870-8421; E-mail: luca.gianni@fondazionemichelangelo.org; and Giampaolo Bianchini, Department of Medical Oncology, IRCCS San Raffaele Scientific Institute, Via Olgettina, 60, Milan 20132, Italy. Phone: 3902-2643-6530; E-mail: giampaolo.bianchini@hsr.it

Clin Cancer Res 2022;28:2167–79

doi: 10.1158/1078-0432.CCR-21-3185

Translational Relevance

In HR-positive (HR^+)/HER2-positive ($HER2^+$) breast cancer, endocrine therapy has limited efficacy, and addition of anti-HER2 drugs leads in general to modest therapeutic improvement, suggesting that the cross-talk between HER2 and estrogen receptor (ER) is bypassed by alternative escape pathways.

We demonstrated, in different breast cancer cell lines, that cotargeting Rb by CDK4/6 inhibition voids the escape mechanisms induced by ER/HER2 cross-talk and triggers the transition from cell quiescence to sustained senescence. These findings were consistent with those observed in the NA-PHER2 trial which enrolled patients with ER^+/$HER2^+$ breast cancer treated with neoadjuvant chemo-free combination of drugs targeting ER, HER2, and CDK4/6-Rb. Our results provide a mechanistic interpretation of the increased clinical activity observed with this combination in NA-PHER2 and MONARCHer studies and provide a support for further development on this therapeutic strategy. In addition, these findings support the ongoing research of biomarkers research to predict for sustained tumor senescence in individual patients.

The convergence of HER2 and ER signals on Rb suggested that pharmacologic block of the triple-way cross-talk with drugs interfering with each individual target might result in therapeutic synergy. In the NA-PHER2 neoadjuvant trial (20) there was a clear indication that therapy consisting of fulvestrant to block ER, palbociclib to block CDK4/6-Rb, and trastuzumab plus pertuzumab to block HER2 was very active in ER^+/$HER2^+$ breast cancer.

In parallel with the aforementioned clinical study, we investigated the effects of the triple block of HER2, ER, and CDK4/6-Rb in a panel of breast cancer cell lines to assess the presence and extent of synergy, and to investigate the underlying mechanisms of interaction. We report here that sustained senescence is a key mechanism of the antiproliferative activity induced by concomitant targeting of ER, CDK4/6-Rb, and HER2 in cell lines and demonstrate, by RNA-sequencing (RNA-seq) of breast cancer biopsies, that senescence is also present and prominent upon exposure to the triple block of patients enrolled in NA-PHER2 trial and associated with retained Ki-67 downregulation.

Materials and Methods

Cell lines

BT474 (catalog no. HTB-20), ZR-75–30 (catalog no. CRL-1504), MDA-MB-361 (catalog no. HTB-27, RRID:CVCL_0620), MCF7 (catalog no. HTB-22, RRID:CVCL_0031), T47D (catalog no. HTB-133), SKBr3 (catalog no. HTB-30), were purchased from ATCC in January 2016. KPL4 were a gift from Prof. Kurebayashi (Japan; Supplementary Table S1). The cells lines from ATCC were guarantees for origin, authenticity, and absence of *Mycoplasma*. Cells were cultured in high-glucose DMEM or RPMI (Lonza) containing 10% FBS (Invitrogen) and 1% penicillin/streptomycin (10.000 UI/mL; Invitrogen) in compliance with ATCC technical data sheet. Cell lines were grown in a humidified incubator at 37°C with 5% CO_2 and regularly checked (approximately every 2/3 months) for any contamination by *Mycoplasma*. For this purpose, the commercial kit MycoAlertTM PLUS Mycoplasma Detection Kit (10 tests) was used (catalog no. LT07–701; Lonza). Usually in our laboratory cell lines were used within 20 to 25 passages of thawing and continuously cultured for less than 6 months.

Reagents

Palbociclib and fulvestrant were respectively from Santa Cruz and Sigma-Aldrich and dissolved in water and in DMSO. Trastuzumab and pertuzumab were from Roche.

Viability

Cells (1,000–6,000) were plated in 96–flat bottom–well plates (Corning), grown overnight, and treated (in triplicate or quadruplicate) with individual drugs or combinations for 72 hours, when 30 μL per well of MTT [3-(4,5-dimethylthiazol-2-yl)-2,5-diphenyltetrazolium bromide; Sigma-Aldrich] were added. After incubation at 37°C for 4 hours, the supernatant was removed and the MTT formazan salt was dissolved in 100 μL of DMSO (Sigma-Aldrich). Absorbance was read at 570 nm using a reference wavelength of 630 nm.

Proliferation

Cells (1×10^5–7×10^5) were plated in a six-wells plate and treated as described above for 72 hours. After drug removal, residual viable cells were allowed to recover and grow for additional 7 days [wash-out period (WO)]. Cell viability was evaluated by Trypan Blue Vitality test at end of treatment (EOT; 72 hours), at day 3, and day 7 of WO.

Western blotting

Cells were lysed with RIPA buffer and proteins were separated on SDS-PAGE using acrylamide fixed-percentage or gradient precast gels (Mini Protean TGX, Bio-Rad). Blotting was performed by a semidry system (Trans Blot Turbo; Bio-Rad). Membranes were subjected to immunoblotting with different primary antibodies of interest listed in Supplementary Fig. S1. Chemiluminescent detection was performed by ECL Clarity reagent (Bio-Rad).

Morphology

3×10^5 cells were plated in six-well plates, treated the day after with single drugs or combinations and let grow for 6 to 12 days. Images were acquired with an inverted microscope IMAGER M2 (Zeiss Oberkochen) at intervals during incubation.

Senescence-associated β-galactosidase

Three different assays were used to observe and quantify senescent cells: (i) colorimetric test (Abcam Senescence Detection Kit) for microscope observation; (ii) Fluorometric Quantitative Cellular Senescence Assay Kit (Cell BioLabs) for a quantitative flow cytometric measurement (Canto II, Beckton Dickinson) of senescence-associated β-galactosidase (SA β-gal) activity; (iii) after staining with the colorimetric kit (Abcam), positive cells were counted by Amnis ImageStreamX (Merck). All methods were used according to the manufacturer's standard protocol.

Cell cycle

1×10^6 cells were plated in 25-cm^2 flasks and treated for 72 hours before detachment by trypsinization. After washing with PBS, cell pellet was incubated with propidium iodide (25 μg/mL), RNase A (0.5 U/mL), and Nonidet P-40 [5% volume for volume (v/v)] in a final volume of 0.5 mL for 30 minutes in the dark before analysis by flow cytometer (FACSCanto II, BD Biosciences). The percentage of cells in G_0–G_1, S, and G_2–M was determined by the data-analysis software FCS Express (De Novo Software).

Apoptosis

Cells were plated and treated as described for cell cycle analysis but, after treatment, all cells were collected including those in culture

medium. Apoptosis was detected by FACSCanto II using the kit Annexin V-FITC/Propidium Iodide (Bender Med-System). The protocol provided by the manufacturer was followed.

Statistical analysis

Statistical analysis was performed using Kruskal–Wallis test followed by multiple comparison by Wilcoxon paired or unpaired test with R software 4.0.1 "See Things Now" (R Development Core Team) and nonparametric Mann–Whitney test (two-tailed) with PRISM RRID:SCR_005375 software v6 (GraphPad Prism RRID:SCR_002798).

Synergism analysis

Synergism of treatments was evaluated according to Bliss independence method (21), where the expected response is a multiplicative effect as if the two drugs acted independently. The percentage of cell survival for each drug was measured by MTT assay, whereas the percentage of surviving cells expected in case of independence was calculated according to the Bliss equation (example for 2 drugs, A and B):

$$Fu_C = fu_A \times fu_B$$

where fu_C is the expected fraction of cell unaffected by combination treatment in case of additivity, and fu_A and fu_B are the fraction of cells unaffected by treatment A and B respectively. The percent difference between Observed and Expected values represents the grade of interaction among drugs. The Bliss equation could also be applied to more than two drugs. The interpretation of Bliss values was: <−10% = trend to antagonism; ±10% = additivity; 10% to 20% = trend to synergism; >20% = synergism. Data from matrices were analyzed by Bliss independence model using the web software SynergyFinder (ref. 22; https://synergyfinder.fimm.fi).

Analysis in patient samples

Patients ($n = 30$) enrolled in NA-PHER2 trial and with centrally confirmed ER^+ (>10%) and $HER2^+$ breast cancer were treated with neoadjuvant trastuzumab, pertuzumab, palbociclib, and fulvestrant. The study was undertaken according to Good Clinical Practice guidelines and the Declaration of Helsinki. All patients provided written informed consent for participation in the study and for provision of tumour tissue for assessment of Ki67 values and for RNA-seq analysis. The study protocol and informed consent form (and any modifications thereof) were approved by independent ethics committees at every participating institution and the relevant competent authority. Ki67-positive cells in tumor were assessed by IHC using MIB-1 antibody (Dako, Agilent Technologies) in a central lab as already reported (20). RNA-seq was performed on core-biopsies obtained pretreatment, at week 2, and on residual disease at surgery (Supplementary Methods for details).

We investigated biomarker dynamics and association with Ki67 downregulation at week 2 and at surgery. On RNA-seq data were assessed: (i) a proliferation signature based on the expression of mitotic kinases (MKS; ref. 23); (ii) a manually curated Senescence Signature (Supplementary Table S2) created after literature search with the aim to select the high relevant markers of senescence at protein and RNA expression level; this gene set (40 genes) was validated using the free database "Senequest" (24) to weigh the genes by number of citations and to determine the expected direction of their modulation during senescence; (iii) the HALLMARK_MTORC1_SIGNALLING gene set (http://www.gsea-msigdb.org/gsea/msigdb/cards/HALLMARK_MTORC1_SIGNALING.html). Single sample gene set scores were computed using the singscore approach (25). Statistically significant differences were assessed by two-tailed Wilcoxon test (paired or unpaired; $P < 0.05$). Gene expression data, relative to all gene sets, are available in Supplementary Table S3.

Availability of data and materials

All the gene expression profiles used in this work have been made available as supplementary information. All the data used in this work can be available upon reasonable request through the corresponding authors.

Results

Cell lines

We selected cell lines with different combinations of HR and HER2 expression (Supplementary Table S1). MDA-MB-361, BT474, and ZR-75–30 have high expression of HER2 and of ER and/or of progesterone receptor (PR). We also selected two control cell lines with HER2 amplification in the absence of HR expression (SKBr3, KPL4), and two control cell lines with normal/low HER2 and HR expression (MCF7 and T47D; Supplementary Table S1). In Supplementary Material we report all experiments conducted to confirm the molecular classification of the selected cell lines (Supplementary Fig. S1A), the expression of relevant proteins affected by the tested drugs (EGFR, HER3, HER4, IGFR, and C-MET, Rb, Cyclin D, Cyclin E1 and E2, CDK4, CDK6, CDKis, p53, MDM2, c-Myc, Bcl-2, Ki67; Supplementary Fig. S1B) and the sensitivity of each cell line to the individual drugs [palbociclib (P; ref. 26), fulvestrant (F), and the anti-HER2 antibodies trastuzumab (H) and pertuzumab (Pert); Supplementary Table S1; Supplementary Figs. S2 and S3].

Studies of the combination(s) of palbociclib, fulvestrant, trastuzumab, and pertuzumab were conducted in cell lines with ER and HER2 overexpression (MDA-MB-361, BT474, ZR-75–30) by exposure for 72 hours to concentrations previously identified as optimal for *in vitro* evaluation of a four drugs combination [P (0.1 μmol/L), F (1 μmol/L), H (20 μg/mL), Pert (25 μg/mL)] taking into account also available information regarding plasma levels or active concentrations in human, and the growth inhibitory activity evaluated *in vitro* by the dose/response curve (Supplementary Methos for details). In ER^+/$HER2^+$ cell lines the combination PFHPert had high antitumor activity (**Fig. 1A**). In BT474 and ZR-75–30 the presence of the anti-HER2 therapy is needed for maximal activity (**Fig. 1B**) and the dual HER2 block with trastuzumab and pertuzumab was superior to trastuzumab only (**Fig. 1C**). In MDA-MB-361, which is relatively resistant to HER2-directed treatments, the addition of fulvestrant was needed for the maximal activity of the four drugs (**Fig. 1B**) and cotreatment with pertuzumab did not lead to more activity than obtained by trastuzumab (**Fig. 1C**).

The possible synergistic effect of double-triple-quadruple combinations at fixed doses of each drug was assessed at 72 hours applying the Bliss independence model (**Fig. 1D**). After treating cells with single agents (palbociclib, fulvestrant trastuzumab, and pertuzumab) and combinations, we measured the cytotoxicity effects by MTT assay. We applied the equation reported in Materials and Methods to calculate the percentage of deviation between the Observed and the Expected effects (% Bliss). The cut-off values are indicated in **Fig. 1D**. Among the $HER2^+$ cells, only the three drugs combination palbociclib/fulvestrant/trastuzumab (PFH) was synergistic in ZR-75–30 (Bliss > 20%) and the quadruple combination PFHPert showed a more than additive effect (Bliss 12%). The same PFHPert combination was only additive in MDA-MB-361 (Bliss 7%) and BT474 (Bliss - 4%) being the Bliss score in the range of additivity, between −10% to +10% (**Fig. 1D**).

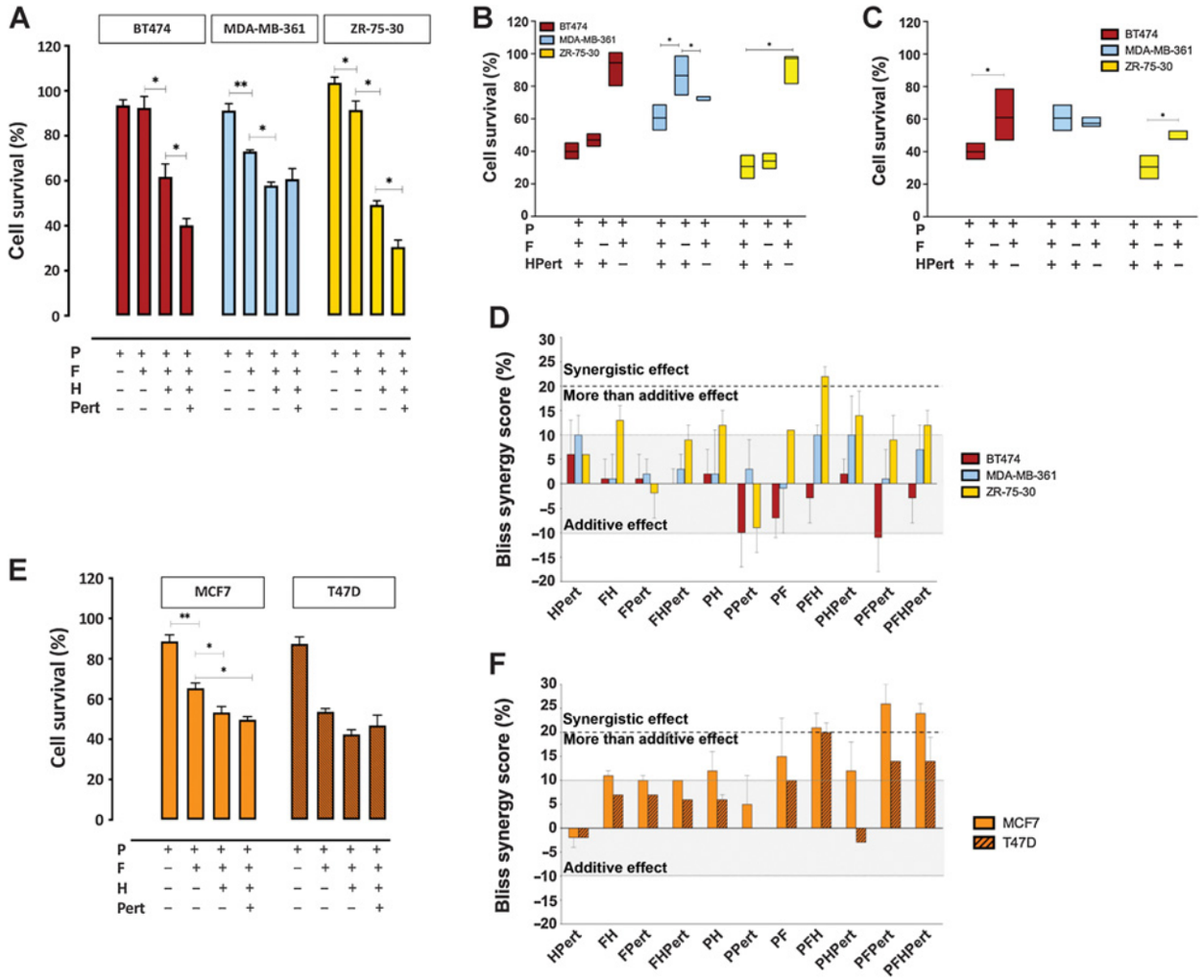

Figure 1.

Drug combinations. **A,** Percent of cell survival by the MTT cytotoxicity assay after 72-hour exposure to palbociclib (0.1 μmol/L), fulvestrant (1 μmol/L), trastuzumab (20 μg/mL), and pertuzumab (25 μg/mL) and their combinations in BT474 (red bars), MDA-MB-361 (light blue bars), and ZR-75–30 (yellow bars). **B,** Contribute of fulvestrant or anti-HER2 therapy to the four drugs combination in the different HER2$^+$ cell lines: the percentage of cell survival, measured by MTT, after 72 hours of P + F + HPert was directly compared with the treatment P + HPert (minus F) and P + F (minus HPert) for BT474, MDA-MB-361, and ZR-75–30. **C,** Contribute of Pertuzumab to the 4 drugs combination in the different HER2$^+$ cell lines: the percentage of cell survival after 72 hours of PFH + Pert was directly compared with the treatment PFH (minus Pert). **D,** Percent Bliss synergy score calculated for each combination. Values from -10% up to 10% (grey area) correspond to additivity; the area from 10% to 20% (dashed bold line) corresponds to a more than additive effect; the area above the dashed bold line at 20% corresponds to synergism. **E,** Percent survival by MTT assay and **F,** Percent Bliss synergy score in HER2^{low} MCF7 (orange bars) and T47D cells (brown bars). Data are mean values of three or more experiments ± SEM; *P* values by Kruskal–Wallis test (multiple comparison by Wilcoxon unpaired test) are reported only for the drugs combination relevant for synergism evaluation. *, $P \le 0.05$; **, $P < 0.01$.

Interaction matrices were performed to study drug combinations in a wide range of concentrations of each agent. Cell survival data from MTT assay were analyzed by the Bliss model and synergy scores were plotted in 2D and 3D maps. An illustrative example is shown in Supplementary Fig. S4 where palbociclib, fulvestrant, and palbociclib/fulvestrant were combined with trastuzumab + pertuzumab (HPert): the Bliss score of maximal drug interaction (5.83%, 10.31%, and 7.63% in BT474, MDA-MB-361, and ZR-75–30, respectively) confirmed the single concentration results.

Combinations of palbociclib, fulvestrant, trastuzumab, and pertuzumab were also tested in the HER2-expressing but not amplified/overexpressed (HER2^{low}) control cells. Unexpectedly, the interaction analysis (**Fig. 1E** and **F**) showed that in MCF7 and T47D the Bliss score reached the synergy cut-off of 20% for the three drug combinations PFH, while PFPert and PFHPert showed a score larger than 20% in MCF7 only. Observation was confirmed in 2D and 3D maps (Supplementary Fig. S4).

Finally, in the HER2$^+$ and HR$^-$ SKBr3 and KPL4 cells (Supplementary Fig. S5A and S5B) the PFH combination showed a more than additive inhibition of proliferation (Bliss between 13% and 17%).

In summary, the quadruple combination of palbociclib, fulvestrant, trastuzumab, and pertuzumab (PFHPert) had additive or more than additive effects in all three ER$^+$/HER2$^+$ cell lines despite their heterogeneous sensitivity to the individual agents. Combined

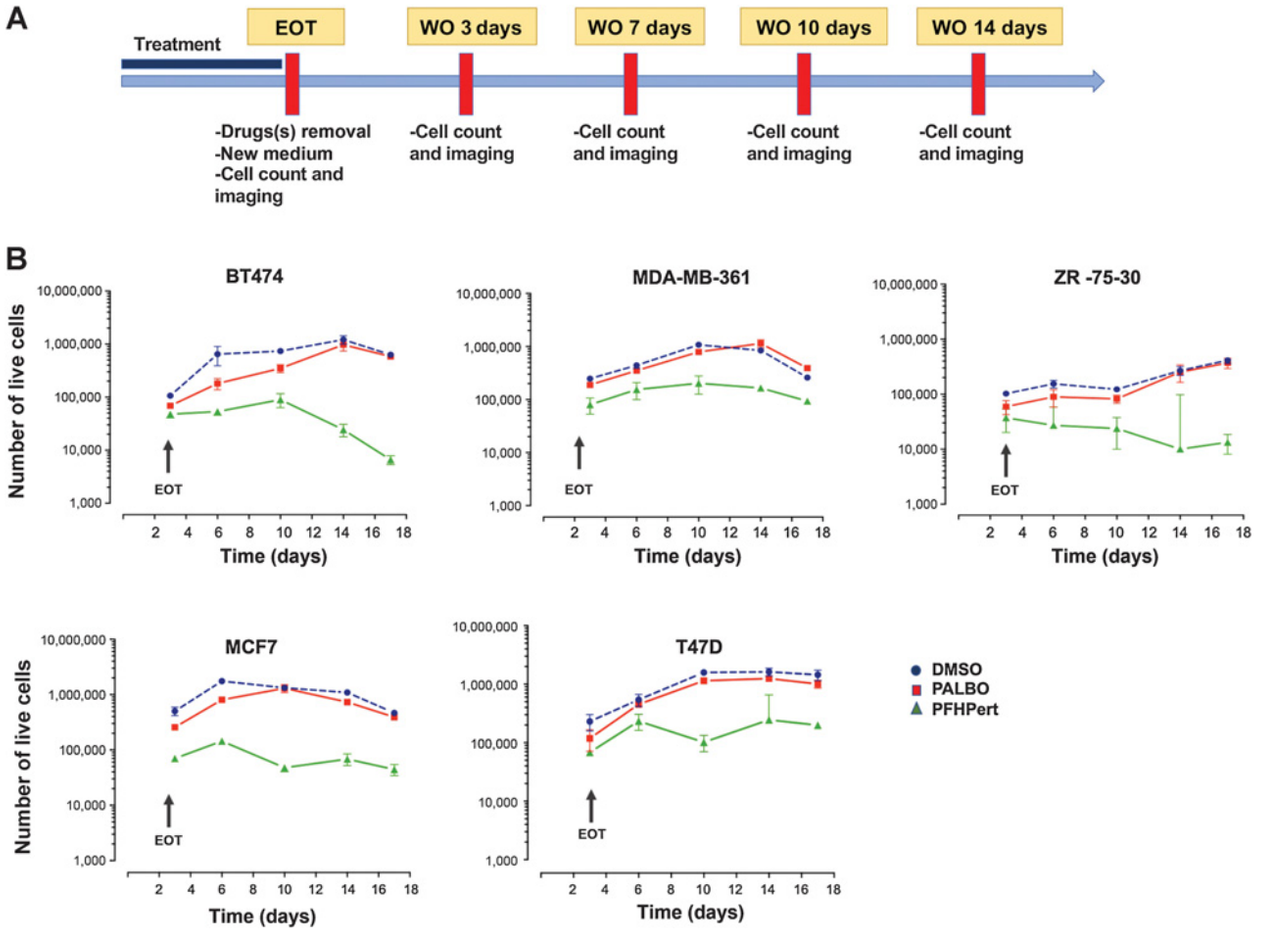

Figure 2.

Long-term survival pattern. **A,** Graphical representation of the treatment schedule adopted to study long-term effects after EOT in the WO. After 72 hours of treatment, drugs were removed and replaced with fresh medium. At EOT and during the WO (till 14 days after treatment) cells were counted and imaging for morphology and SA β-gal expression was taken. **B,** Kinetics of cell counts by Trypan Blue, from EOT up to day 14 of WO. The results of DMSO control (blue circle), palbociclib (PALBO) alone (red square), and PFHPert treatment (green triangle) were showed. In the top panels are the results for the $HER2^{+}$ cell lines (BT474, MDA-MB-361, ZR-75-30). In the bottom panels are the results for the $HER2^{low}$ cell lines (MCF7, T47D). Data are mean ± SEM from at least three experiments.

with palbociclib and fulvestrant, in the cells sensitive to anti-HER2 therapy BT474 and ZR-75–30, dual block of HER2 with trastuzumab and pertuzumab led to an increased effect on cell survival compared with trastuzumab alone. The presence of fulvestrant was key for maximal activity in MDA-MB-361. Notably, the combinations including single or dual block of HER2 were synergistic in $HER2^{low}$ cells.

Long-term effects

All agents used in the experiments have mostly cytostatic activity. We therefore explored the long-term effects and patterns of regrowth in residual cells after the 3-day exposure with each drug (palbociclib, fulvestrant, trastuzumab, pertuzumab) alone and for different combinations. Briefly, at the end of 72 hours of exposure [end of treatment (EOT)] drugs were removed, fresh medium was added once, and cultures continued for additional 14 days of WO. As shown in **Fig. 2A** cell growth was monitored by cell counting and morphologic imaging in bright field (BF).

Figure 2B shows cell counts normalized for counts at EOT during the 14-day WO. In all cell lines single agent palbociclib blocked cell proliferation in presence of the drug but growth resumed after palbociclib removal with a rate similar to untreated control. PFHPert blocked or greatly limited cell regrowth in $HER2^{+}$ and in $HER2^{low}$ cells with the exception of the anti-HER2 resistant cell lines MDA-MB-361. The MDA-MB-361 cells treated with the PFHP combination show a growth curve that, up to 14 days posttreatment, retains a regrowth profile similar to that of untreated cells (DMSO) showing a delta value of about 65% between DMSO and PFHPert groups. In the other cell lines BT474, ZR-75–30, MCF7, and T47D the delta was 98%, 96%, 90%, and 86.4% respectively.

A clear senescence-like phenotype was observed at the end of the 72-hour treatment in BT474 and MCF7 (as example of $HER2^{+}$ and $HER2^{low}$ cells; **Fig. 3A**); indeed cells showed altered morphology, flattening, and increased cell area (**Fig. 3B**). These observations are in agreement with the already known "senescence-like phenotype" induced by CDK4/6 inhibitors (19, 27, 28). As for classical senescence,

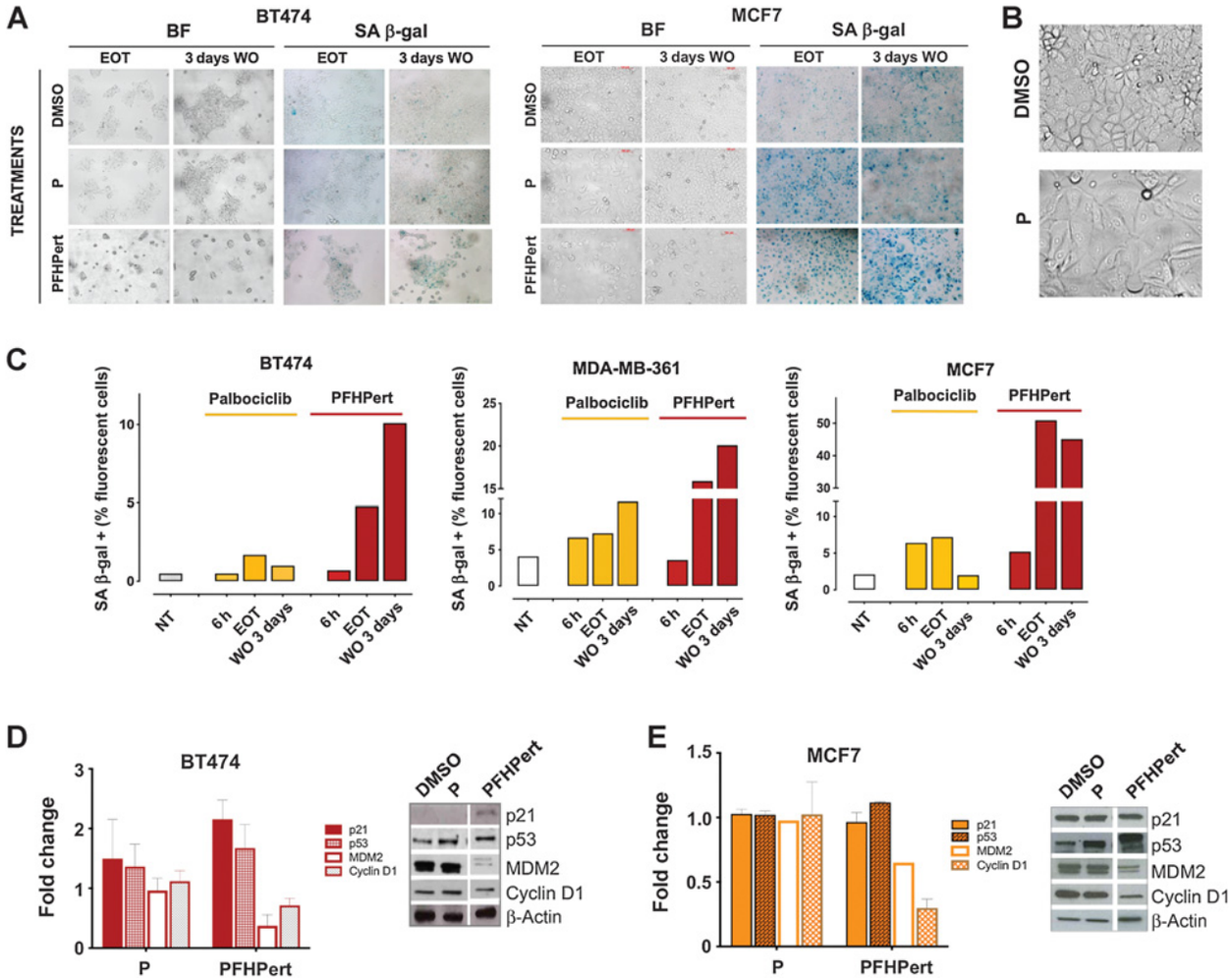

Figure 3.

Senescence. **A,** Study of the senescence-like phenotype in HER2^{+} BT474 cell line, and in HER2^{low} MCF7 cell line. The effects of treatments with palbociclib and PFHPert were studied at EOT (72 hours) and after additional 3 days of WO with fresh medium. Morphologic changes after WO were shown in BF images on the left-sided panels. In the right-sided panels the SA β-gal enzyme activation in the same conditions was shown. For the complete panel of treatments in BT474, MCF7, and MDA-MB-361 see Supplementary Fig. S6. **B,** Representative images of morphologic changes in MCF7 cell treated with palbociclib for 72 hours. **C,** Evaluation of SA β-gal activation at baseline (untreated cells), during (6 hours), at the end (EOT), and after treatment (3 days WO) in BT474 (graph on the left), MDA-MB-361 (graph on the middle), and MCF7 (graph on the right). The comparison between untreated cells (white bars), palbociclib alone (yellow bars), and PFHPert (red bars) was reported. Staining was performed with a colorimetric kit and detection of % of SA β-gal–positive cells was evaluated by Amnis ImageStreamX Flow Cytometry Technology (Merck). Modulation of p53-p21-MDM2 axis and Cyclin D1 during treatment with palbociclib and PFHPert in BT474 (**D**) and MCF7 (**E**). Data are from two or three replicates but only one representative blot is showed. Values were calculated after correction for the loading marker and normalization by the control sample in DMSO. Bars represent the mean ± SEM. NT, untreated cells; h, hours.

we found that cells treated with palbociclib for 72 hours showed an activation of the SA β-gal (**Fig. 3A**). However, after palbociclib removal (3 days WO) cells reverted to the original appearance and the activity of SA β-gal decreased. Reversal of the senescence-like phenotype did not occur when palbociclib was combined with fulvestrant and the anti-HER2 antibodies (PFHPert). Senescence was also quantified by a cytofluorimetric test, by which we confirmed the colorimetric data and demonstrated that the activation of SA β-gal during the different treatments shows a continuous increase over time. Representative results in MCF7 are reported in Supplementary Fig. S5C. Supplementary Figure S6 shows additional images of senescence in BT474 and MCF7, and the results in MDA-MB-361. Quantification by ImageStream (**Fig. 3C**) reconfirmed the activation of SA β-gal during palbociclib treatment (6 hours and EOT) and a reversal after treatment (WO 3 days) in BT474 and MCF7. Following PFHPert the percentage of SA β-gal–positive cells was higher than after palbociclib alone and, after day 3 of WO, such percentage (10%, 20%, and 50% in BT474, MDA-MB-361, and MCF7 respectively) was maintained.

To dissect which, among the multiple pathways involved in cellular senescence, underlies the transition from reversible to sustained senescence we observed, we investigated those involving cell-cycle regulation and relying on the Cyclin D1-p21-p53 axis. We found that, in BT474, the addition of fulvestrant, trastuzumab, and pertuzumab to palbociclib promoted a 2.1-fold induction of the CDK regulators p21WAF1/Cip1 and 1.6-fold induction of p53 (**Fig. 3D**). This event

was associated with 50% reduction of MDM2 and Cyclin D1. Similar results were observed in MCF7, although to a lesser extent (**Fig. 3E**).

We tested whether apoptosis was involved as outcome of the sustained senescence (Supplementary Fig. S7A). In MDA-MB-361 and MCF7 the percent of apoptotic cells was no different from that of untreated cells. In BT474 only, apoptosis was induced with HPert treatment.

In summary, palbociclib induced an SA β-gal expressing-senescence phenotype that was reversible after drug removal and consistent with a quiescence status. In contrast, the addition of fulvestrant, trastuzumab, and pertuzumab to palbociclib led to a more profound and sustained senescence effect.

Pharmacodynamics in HR$^+$/HER2$^+$ cells

Given the complex interplay between ER, HER2, and Rb, we tested the effect of the individual drugs and combinations on their intracellular targets. Western analysis showed that 72-hour exposure to fulvestrant (1 μmol/L) led to the expected degradation of ERα, the progesterone receptors PR A/B, and IGF-IRβ proteins (Supplementary Fig. S7B). This effect was observed in all combinations that included fulvestrant. Of note, in MDA-MB-361 the fulvestrant-induced down-modulation was more pronounced for PR than for ERα.

In BT474 and ZR-75–30, but not in MDA-MB-361, palbociclib (0.1 μmol/L) did not completely inhibit the phosphorylation of Rb while induced Cyclin D1 accumulation. In presence of fulvestrant and palbociclib/fulvestrant combination a hyper-phosphorylation of Rb and hyper-accumulation of Cyclin D1 was observed (Supplementary Fig. S7C). In BT474 and ZR-75–30, after the addition of anti HER2 antibodies, and in MDA-MB-361, after given fulvestrant, the inhibition of Rb phosphorylation was evident and concurrent with the reduction of Rb total protein (Supplementary Fig. S7C), indicating a strong induction of proteomic degradation.

After exposure to palbociclib, fulvestrant, and palbociclib/fulvestrant we also detected increased phosphorylation of EGFR, HER3, and HER2 (**Fig. 4A**; Supplementary Fig. S8A). The increase of pEGFR (Tyr845) and pHER3 (Tyr1289) was more pronounced in BT474 and MDA-MB-361, while induction of pHER2 (Tyr1248) was much more marked in MDA-MB-361 and ZR-75–30. The highest effect was seen in cells exposed to fulvestrant monotherapy and minimal with palbociclib monotherapy. This effect on RTKs of palbociclib/fulvestrant was completely reversed by the addiction of the anti-HER2 doublet trastuzumab/pertuzumab except for EGFR and HER2 in MDA-MB-361 (resistant to HER2-targeted therapies).

Since palbociclib and fulvestrant also influence the mTOR pathway, to explore whether there was a feedback reactivation of EGFR, HER3, and HER2 after treatment with palbociclib and palbociclib/fulvestrant (PF), we investigated the effect of treatments on the Akt/mTOR/S6K&4EBP1 pathway. As expected by functional induction of RTKs, we observed that phospho-Akt (Ser473) increased by about 1.7-fold in ZR-75–30 and 7.5-fold in MDA-MB-361 after PF (**Fig. 4B**; Supplementary Fig. S8B). Addition of trastuzumab/pertuzumab to PF led to the inhibition of AKT phosphorylation in ZR-75–30 cells but not in MDA-MB-361 in analogy with what seen for EGFR and HER2 phosphorylation (**Fig. 4A**). Downstream of mTOR, the phosphorylation of 4EBP1 was significantly reduced during treatments containing the anti-HER2 antibodies (**Fig. 4C**; Supplementary Fig. S8B) in BT474 and ZR-75–30, while phospho-S6K was unaffected (BT474 in Supplementary Fig. S8C).

Taken together these findings indicated that treatment of ER$^+$/HER2$^+$ breast cancer with fulvestrant and even more with palbociclib/fulvestrant combination, promotes the reactivation of the ErbB-family of receptors probably due to the induction of Akt/mTOR activity, and that the addition of trastuzumab/pertuzumab to palbociclib/fulvestrant combination blocks this escape mechanism.

Pharmacodynamics in HER2^{low} cells

We observed a fulvestrant-induced degradation of ER, PR A/B, and IGF-IR (Supplementary Fig. S9A; MCF7 only) associated to an increased phosphorylation of the RTKs also in HR$^+$/HER2^{low} MCF7 and T47D cells (Supplementary Fig. S9B). MCF7 and T47D had low baseline levels of EGFR and HER2 protein (phosphorylated and total) and high levels of total HER3, but not of pHER3 (Supplementary Fig. S1). Also, in HER2^{low} the contribution of palbociclib in RTKs rebound was minimal but fulvestrant, and more strongly palbociclib/fulvestrant combination, induced phosphorylation of EGFR and HER3 up to eight- to nine-fold the level in basal conditions. The addition of the anti-HER2 antibodies prevented or reduced the phosphorylation of both receptors, in line with the unexpected synergism of PFHPert. In HER2^{low} cells exposure to palbociclib, fulvestrant, and their combination not only triggered the activation of HER2, but also led to overexpression of total HER2 protein (Supplementary Fig. S9B).

In MCF7 palbociclib/fulvestrant treatment was associated with an increased phosphorylation of Akt (Supplementary Fig. S9A and S9C) and the more pronounced effects on mTOR pathway (p4EBP1 reduction) were observed when the anti-HER2 antibodies were added to palbociclib/fulvestrant (Supplementary Fig. S9C), while pS6K was again unaffected (Supplementary Figs. S8C and S9A).

In summary, in the HER2^{low} MCF7 and T47D cells we observed an induction of ErbB receptors after fulvestrant and fulvestrant/palbociclib similar to that we described in HER2$^+$ cells suggesting an expression induction and functional activation of RTKs also in cells with a basal low expression.

RNA-seq of tumor biopsies from NA-PHER2 patients

In the NA-PHER2 trial, women with ER$^+$/HER2$^+$ early breast cancer received the PFHPert regimen for five cycles before surgery (20). The primary endpoint of this study was Ki-67 downregulation at week 2. We performed RNA-seq on samples collected pretreatment ($n = 28/30$; 93.3%], at week 2 ($n = 24/30$; 80.0%) and on surgical specimen in patients with residual disease ($n = 20/22$; 90.9%). In this biomarker population, a significant reduction ($P = 1.2e^{-4}$) of Ki67 was observed at week 2 similarly to the overall study population (**Fig. 5A**). Using the validated cut-off value of 10%, two subgroups of patients were defined: endocrine sensitive [<10%; low Ki67 detected at week 2 (Ki67-w2)] and endocrine resistant (≥10%; high Ki67-w2). The decreased tumor cell proliferation was also confirmed by testing the MKS proliferation signature (ref. 23; $P = 3.3e^{-6}$; **Fig. 5B**; Supplementary Table S2). The Senescence Signature score (Supplementary Tables S1 and S2) significantly increased from baseline to week 2 (**Fig. 5C**) in almost all patients, however at week 2 this score was significantly higher in patients with low than high Ki67-w2 ($P = 7.7e^{-4}$; **Fig. 5D**). The 5 patients who had pathologic complete response (pCR) at surgery, had a similar pattern of correlation compared with patients with residual disease (data not shown).

A similar analysis was performed considering Ki67 measured in the time interval from week 2 to surgery (**Fig. 6A**). Two groups were defined according to 10% cut-off at surgery. High Ki67 detected at surgery (Ki67-surg) included patients without early Ki67 downregulation, but also patients with Ki67 rebound after decrease at week 2, whereas low Ki67-surg was associated with maintained downregulation. Rebound was not associated with the interval between treatment

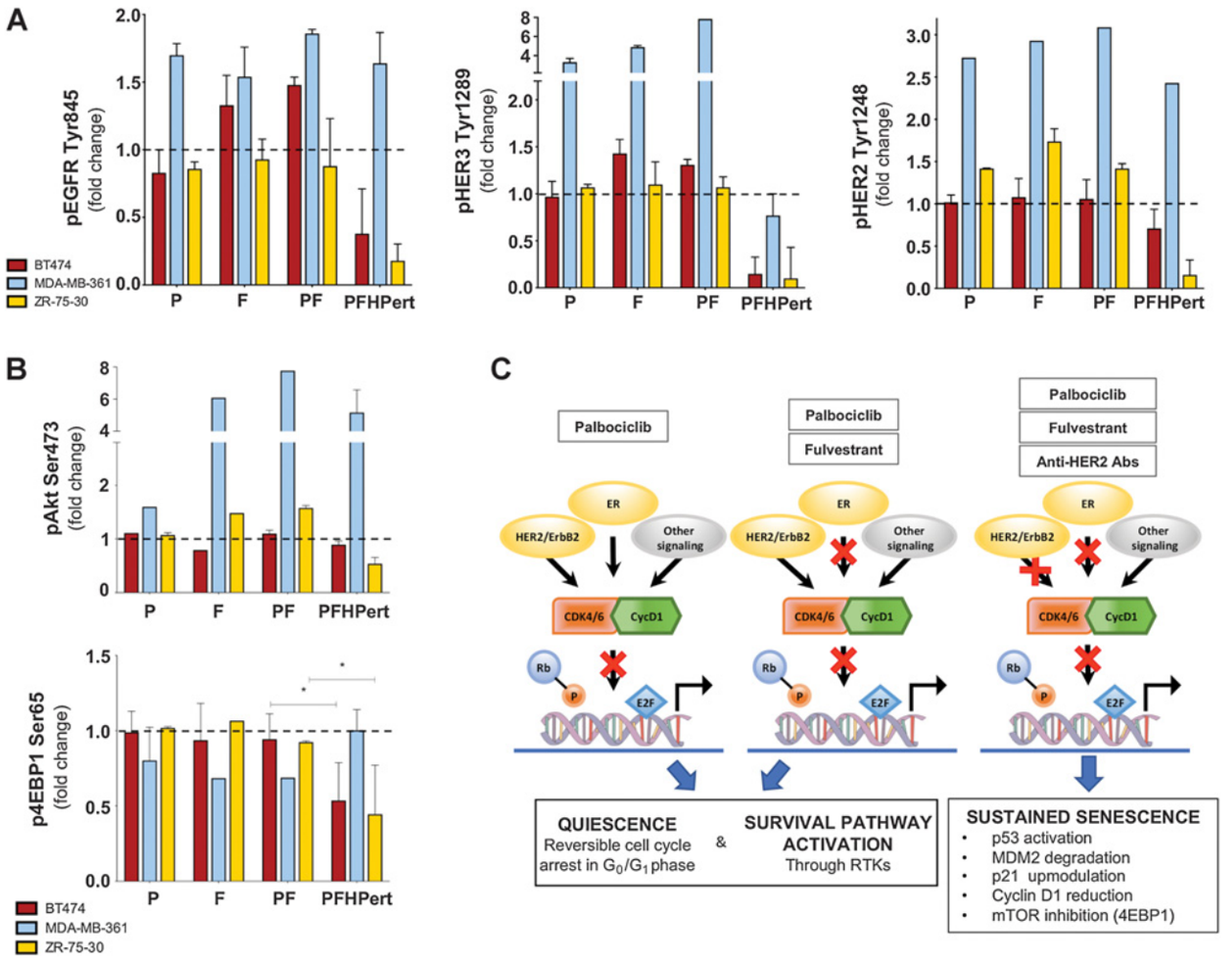

Figure 4.

ErbB receptors modulation in ER$^+$/HER2$^+$ cell lines and study of pathways involved in ER/HER2/Rb cross-talk. **A,** Quantification of Western blot bands (see Supplementary material for details) for the ErbB receptors (left panel pEGFR Tyr845, middle panel pHER3 Tyr1289, and right panel pHER2 Tyr1248) in BT474 (red bars), MDA-MB-361 (light blue bars), and ZR-75–30 (yellow bars) after 72 hours of treatment with P, F, PF, and PFHPert. **B,** Quantification of the Western blot bands of phosphorylated Akt (Ser473; top panel) and 4EBP1 (Ser65; bottom panel). **A** and **B,** Dotted lines indicate the reference ratio in DMSO. Data were mean ± SEM of two or three experiments and in Supplementary Fig. S8 only one representative blot was showed. *P* value by Mann–Whitney test, two-tailed (*, $P \le 0.05$). All values were calculated after correction for the loading marker (β-actin or GADPH) and normalization by the control sample in DMSO. **C,** Summary of the effects of treatments with palbociclib (left panel), palbociclib/fulvestrant (middle panel), and PFHPert (right panel) on their molecular targets and on the different observed outcomes (blue arrow) in HER2$^+$ and in HER2^{low} breast cancer cells. Exposure to palbociclib and palbociclib/fulvestrant promotes a quiescence status in G_0 or G_0–G_1 that shares the features with a senescence status that is transient and reversible after drug removal. In this condition, a survival pathway is induced through reactivation of the RTKs/Akt/mTOR axis. Addition of anti-HER2 drugs blocks this escape and promotes sustained senescence (characterized by p53 activation, MDM2 degradation, p21 upmodulation, Cyclin D1 reduction, and mTOR inhibition). This scheme applies to breast cancer cells carrying either a constitutive (HER2 amplification/overexpression) or a functionally inducible (HER2^{low} cells) activation of the ErbB family of receptors. Abs, antibodies.

discontinuation and surgery (1–6 weeks; ref. 20). In low Ki67-surg patients the Senescence Signature score was maintained high in the interval between week 2 and surgery (**Fig. 6B**, left panel) differently from the patients with high Ki67-surg who had a significant decrease of expression of Senescence genes ($P = 4.9e\text{-}3$; **Fig. 6B**, right panel). This observation was highlighted in **Fig. 6C** and **D** in which both the variation of the Senescence Signature between week 2 and surgery (delta surgery–week2; **Fig. 6C**) and the absolute Senescence Score (**Fig. 6D**) were higher in patients with low compared with high Ki67-surg ($P = 0.015$ and $P = 1.8e^{-4}$, respectively).

To investigate the possible role of mTOR pathway in the context of PFHPert-treated patients, we calculated the single sample enrichment score of the HALLMARK_MTORC1_SIGNALLING gene set in the RNA-seq data (Supplementary Table S2). The dynamics (**Fig. 6E**) showed a signature downmodulation at week 2 followed by a variable rebound at surgery. We found that patients with low Ki67-surg maintained low level of MTORC1 gene set score between week 2 and surgery (**Fig. 6F**, left panel). The delta from surgery to week 2 (**Fig. 6G**) and score (**Fig. 6H**; $P = 0.019$) were higher in the High Ki67-surg group.

In brief, in patients treated with PFHPert an overall early activation of senescence-related genes was observed in the majority of the patients, but this effect was stronger in patients with strong Ki67 downregulation at week 2 and at surgery. Given that drop of Ki67

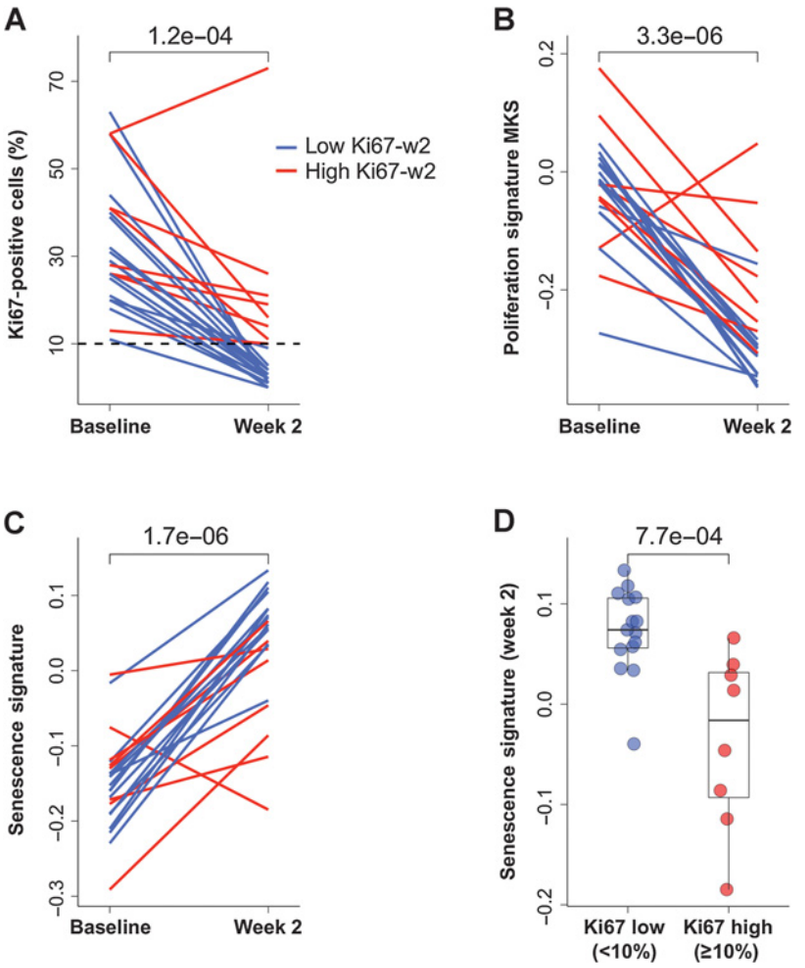

Figure 5.

Proliferation markers and senescence at week 2 in NA-PHER2 patients. **A,** Individual dynamic, from baseline to week 2, of Ki67-positive cells (%) detected by IHC in patients ($n = 22$) treated with palbociclib, fulvestrant, trastuzumab, and pertuzumab (PFHPert). Dashed line represents the cut-off to classify patients with low Ki67-w2 (<10% blue line) or high Ki67-w2 (> = 10% red line). *P* value was assessed by Wilcoxon paired test (two-tailed). **B,** The proliferation signature MKS was tested in RNA-seq data from paired tumor core-biopsies obtained pretreatment and at day 14 ($n = 22$). Data are expressed as dynamic score for individual patients stratified for low (blue line) and high (red line) Ki67-w2. *P* value was by Wilcoxon paired test (two-tailed). **C,** Relationship between Ki67 and senescence gene signature expression during treatment with PFHPert. The dynamics, from baseline to week 2, of the Senescence Signature is reported for patients showing a low (blue line) or high (red line) Ki67-w2. *P* value by Wilcoxon paired test (two-tailed). **D,** Box plot described the correlation between Senescence Signature score at week 2 and level of Ki67 measured at week 2 in the two patient subgroups low Ki67-w2 (blue circles) and high Ki67-w2 (red circles). *P* value was by Wilcoxon unpaired test (two-tailed).

below the 10% threshold at week 2 is a validated surrogate marker of long-term benefit from endocrine therapy (29), we propose that sustained high Senescence Signature during and after treatment with PFHPert linked to the greater antiproliferative effect might be an indicator of long-term benefit. Indeed, activation of MTORC1 pathway was associated with the High Ki67 at surgery and Ki67 rebound, thus confirming its possible role in acquired resistance.

Discussion

In our study we explored the role of cell-cycle regulation through the Rb checkpoint in the context of the well-known cross-talk between the estrogen and the erbB2 receptors (3, 4, 30) in breast cancer cell lines with HER2 gene amplification and ER expression and in patients treated in the NA-PHER2 trial (20). By use of drugs blocking ER (fulvestrant), HER2 (trastuzumab and pertuzumab), and the Rb checkpoint regulation through CDK4/6 (palbociclib) we showed, in cell lines model, that block of Rb and additional block of ER and HER2 signaling triggered sustained senescence, not only in ER^+ and $HER2^+$ cells but also in ER^+ cells formally $HER2^-$, without HER2 amplification/overexpression but with HER2 functionally activable ($HER2^{low}$). We also confirmed, in a companion neoadjuvant clinical trial enrolling women with $HER2^+$ and ER^+ breast cancer (20), that upon exposure to the four drugs combination there was a significant upregulation of a senescence gene signature, and that it was associated with downregulation of Ki67, a hallmark of endocrine sensitivity and long-term benefit from endocrine-based combinations (29, 31). Taken together our findings may have a role in defining new chemotherapy-free therapeutic approaches for breast cancers with ER expression and HER2 amplification or functional activation.

In $HR^+/HER2^+$ cells we documented that concomitant block of ER, HER2, and CDK4/6-Rb pathways has additive to more than additive antiproliferative effects. Using Bliss test (21, 22, 31, 32) we showed that the effect of palbociclib was greatly enhanced with relevant distinct features. In cells sensitive to anti-HER2 therapy the concomitant block of CDK4/6 and of HER2 voided any additional effect from fulvestrant, as if blocking of ER signaling was redundant to sustain survival in the context of the concomitant inhibition of HER2 and CDK4/6. In MDA-MB-361($HR^+/HER2^+$ cells resistant to HER2-directed therapies), the addition of fulvestrant was instead key to achieve maximal activity, suggesting that, in $HER2^+$ cells resistant to modulation of HER2, the dependence of cell survival on ER signaling is crucial and the block of ER signaling is a requisite to reach additive interaction with block of Rb and Cyclin D1.

Thereafter, we investigated whether the synergy rely depended on an incremental cytostatic effect or on other mechanisms. The assay we developed measured cell survival and several markers of senescence

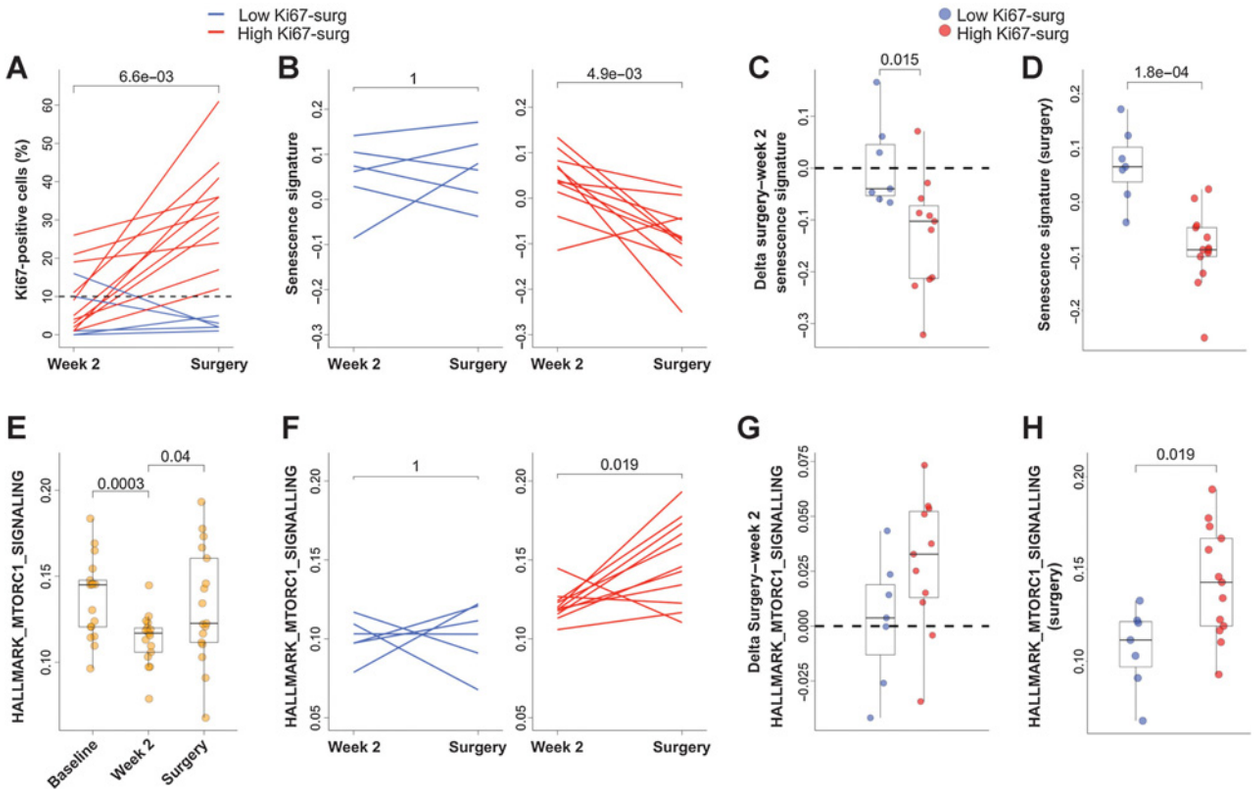

Figure 6.

Proliferation markers and senescence at surgery in NA-PHER2 patients. **A,** Individual dynamic, from week 2 to time of surgery in residual disease, of Ki67-positive cells (%) detected by IHC in tumors biopsies of patients ($n = 17$) treated with palbociclib, fulvestrant, trastuzumab, and pertuzumab (PFHPert). Patients with low (<10%; blue line) or high Ki67-w2 (≥10%; red line) were reported. Note that levels of Ki67 were not associated with time interval between treatment discontinuation and surgery. Dashed line represents the 10% cut-off. *P* by Wilcoxon paired test (two tailed). **B,** The dynamic of Senescence Signature score between week2 and surgery was different in patients with low Ki67-surg (blue line, left panel) and in the patients with high Ki67-surg (red line, right panel). *P* value by Wilcoxon paired test (two-tailed). box plots show, respectively, that both the Delta Senescence Signature (surgery—week 2; **C**, $n = 18$) and the absolute score values (**D**, $n = 20$) of Senescence Signature were significantly different between patients with low Ki67-surg (blue circles) and with high Ki67-surg (red circles). *P* values were by Wilcoxon unpaired test (two-tailed). **E,** Dynamics of HALLMARK_MTORC1_SIGNALLING evaluated in 17 patients with paired samples at baseline, week 2, and surgery ($n = 51$). *P* values were by Wilcoxon unpaired test (two-tailed). **F,** Relationship between Ki67 and MTORC1 pathway during treatment with PFHPert. In the interval between week 2 and surgery, the levels of gene signature HALLMARK_MTORC1_SIGNALLING were maintained low in patients with low Ki67-surg (blue line; left panel) while were significantly upmodulated in patients with high Ki67-surg (red line; right panel). *P* value was by Wilcoxon paired test (two-tailed). **G,** Box plot showing that in patients with low Ki67-surg (blue circles) the delta from surgery to week 2 of HALLMARK_MTORC1_SIGNALLING signature is lower than that measured in patients with high Ki67-surg (red circles), but the difference was not statistically significant ($P = 0.085$). *P* values by Wilcoxon unpaired test (two-tailed). **H,** The absolute HALLMARK_MTORC1_SIGNALLING score detected at surgery was significantly correlated with Ki67-surg. Patients with low Ki67-surg (blue circles) had low levels of MTORC1 signal activation.

and apoptosis at the end of the 72-hour-long drug exposure and for several days after removal of all drugs and continuous culture in optimal growth conditions. The class of CDK4/6 inhibitors leads to cell cycle arrest in G1/G0 and has notably a cytostatic effect (28). As already observed and reported (19, 27), palbociclib monotherapy induced a senescence-like morphology with flattening and increased cell area associated with SA β-gal activation. However, after removal of the drug, there was a regrowth of cells at the rate of untreated controls and an abatement of SA β-gal activation. Exposure to the combination of palbociclib, fulvestrant, and dual block of HER2 was instead associated with no or limited regrowth as expected by the engagement of a sustained senescence (33). However, this effect was heterogeneous among cell lines suggesting an interaction with the molecular context and related to HER2-antibody sensitivity.

Notably, none of the treatments led to any relevant level of apoptosis during the 72 hours of drug exposure, consistently with senescence being the event at the basis of the reported effects on cell survival and synergistic drug interaction.

Some unexpected observation emerged from HER2 not amplified/overexpressing cell lines, which were initially selected as control. While in HR^- SKBr3 and KPL4 the addition of fulvestrant had nil or minimal influence on survival, in the $HER2^{low}$ MCF7 and T47D a very pronounced synergy was observed by concomitant block of ER, HER2, and CDK4/6.

The association of CDK4/6 inhibition and endocrine therapy has set a new standard of treatment in ER^+-positive/$HER2^-$ metastatic breast cancer (13, 14) and several combinations of endocrine therapy and CDK4/6 inhibitors are being tested as adjuvant therapy in early operable breast cancer (5, 14, 15, 18, 34, 35). The rebound of erbB-family receptors has been already observed in vitro after treatment with CDK4/6 inhibitors both in $HER2^+$ (19) and $HER2^{low}$ (36) cells and, as a consequence of the crosstalk between estrogen receptors and erbB

receptors, the rebound was observed after treatment with endocrine therapy (37, 38) and involved different members of erbB receptor family. For both CDK4/6 inhibitors and endocrine therapy, this phenomenon seemed to have a central role in the acquisition of drug resistance. In our experiments we confirm in $ER^+/HER2^{low}$ MCF7 and T47D the efficacy of concomitant fulvestrant/palbociclib, but we also show that the maximal synergy is reached when the anti-HER2 mAbs were added. This is in agreement with the observation of HER2 functional activation that may represent an escape pathway for survival (39–42) in $HER2^+$ and $HER2^{low}$ breast cancer.

Importantly, in $HER2^{low}$ cells the anti-HER2 treatment is key for synergy but is not a substitute for ER-block by fulvestrant, in analogy with the requirement of fulvestrant for maximal effects that we observed in MDA-MB-361 cells that are $HER2^+$ but resistant to HER2-directed antibodies. In those cells maximal effect was concurrent with a strong induction of Rb protein degradation, a well-known mechanism of transcriptional output of RB/E2F target genes regulation induced by CDK4/6i and selective estrogen receptor degrader (43, 44).

We studied the possible markers that describe the transition from the senescence-like/quiescence status to sustained senescence (34, 45–47) that resulted in cell death in $HER2^+$ and $HER2^{low}$ cells. As already known senescence could be triggered by several factors and multiple pathways could be involved. We focused our attention on the specific hallmarks relative to the cell-cycle withdrawal (24). With expected intercell lines variability, the quiescence status was characterized by Cyclin D1 stabilization/accumulation while sustained senescence showed Cyclin D1 reduction, p53 activation, MDM2 degradation, p21 upmodulation, and mTOR inhibition.

Based on the results we propose that a complex interplay regulates the different states of quiescence and sustained senescence in breast cancer cell lines with HR expression and HER2 amplification or functional activation. Such interplay can be exploited as recapitulated in the cartoons of **Fig. 5C**.

Importantly, our *in vitro* findings have consistent correspondence in observations emerged from the trial NA-PHER2, in which we tested the neoadjuvant use of palbociclib, fulvestrant, and trastuzumab with pertuzumab in women with HER2 amplified breast cancer and ER expression and found a major effect on the proliferation marker Ki67 at 2 weeks since starting the combined chemo-free regimen (20). At the same time the drugs led to major clinical objective response in all patients, and to pCR in 27% of them (20).

Gene expression, assessed on core-biopsies from patients enrolled in the trial, showed correspondence between Ki67 measured by IHC and a previously defined gene-expression based proliferation signature (MKS; ref. 23). Senescence was assessed as a 40 genes manually curated signature. High expression of senescence-related signature was detected in patients with low Ki67 both at week 2 and at surgery. The clinical relevance of these two time points for Ki67 assessment as marker of response to endocrine therapy had already been established (30, 48), thus higher senescence is linked with clinically validated surrogates of long treatment benefit.

In cell lines we described a mechanism of escape from the treatment with palbociclib and fulvestrant involving the ErbB-receptors/Akt/mTOR axis reactivation. The addition of trastuzumab and pertuzumab was able to block these events. In line with this observation, in the NA-PHER2 study we found that MTORC1 downmodulation, assessed as HALLMARK_MTORC1_SIGNALLING gene set, was strictly related to low Ki67 at week 2 and at surgery, whereas pathway upregulation was linked to escape and Ki67 rebound at surgery.

Overall, cell and tumor tissue findings of the present report clearly point to a trigger to sustained senescence at week 2 of the NA-PHER2 study by use of concomitant targeting of HER2, Rb, and ER. The findings at surgery should also be interpreted in the light of the variable length of palbociclib discontinuation before surgical sampling, and their full mechanistic relevance for prognosis should wait the results of clinical trials designed for efficacy assessment.

The relevance of targeting Rb regulation by CDK4/6 inhibition while concomitantly targeting the ER and the HER2 signaling finds independent confirmation in the very recent report of the statistically superior benefit associated with use of trastuzumab, fulvestrant, and the CDK4/6i abemaciclib in women with metastatic $ER^+/HER2^+$ tumors in the MONARCHer study (49).

In brief, the findings of the present report contribute to in part clarify the intricate crosstalk between the cell-cycle regulation and the proliferation signals funnelled by the ER and the HER2 pathways. Such complex interaction can be effectively disrupted to enhance the transition from quiescence to sustained senescence in cell lines and patients. The involvement of the MTORC1 pathway, as escape mechanism *in vitro* and *in vivo*, suggest the opportunity to use mTOR inhibitors in combination to overcome treatment resistance. Overall, the findings reported here propose the concomitant blockade of HER2, ER, and CDK4/6-Rb pathway as an effective chemotherapy-free treatment to be tested and they provide a description of mechanisms of sensitivity/resistance to this regimen which could provide insight for further refinement and improvements.

Authors' Disclosures

D. Tosi reports nonfinancial support from MSD, AstraZeneca, Pfizer, Janssen, and Boehringer-Ingelheim, personal fees from Mabqi and Brenus Pharma, and grants from Ipsen and SATT AxLR during the conduct of the study; in addition, D. Tosi has a patent for Association of actives for treating prostate cancer pending. G. Bianchini reports personal fees from Pfizer, Roche, Novartis, Eli Lilly and Company, AstraZeneca, Daiichi Sankyo, and Seagen outside the submitted work. L. Gianni reports grants from Roche, Breast Cancer Research Foundation (BCRF), and Pfizer during the conduct of the study; personal fees from AstraZeneca, Ely Lilly and Company, Roche, Pfizer, Seattle Genentics, Artemida Pharma, Synaffix, Menarini Ricerche, and Biomedical Insights; grants and personal fees from Zymeworks and Revolution Medicine; other support from METIS Precision Medicine, Amgen, and QU Biologics outside the submitted work; in addition, L. Gianni has a patent for EU N. 12195182 issued and a patent for EU N.12196177.5 issued. No disclosures were reported by the other authors.

Authors' Contributions

L. Viganò: Conceptualization, data curation, formal analysis, supervision, validation, investigation, methodology, writing–original draft. **A. Locatelli:** Conceptualization, data curation, formal analysis, supervision, validation, investigation, methodology, writing–original draft. **A. Ulisse:** Data curation, formal analysis, methodology. **B. Galbardi:** Data curation, formal analysis, methodology, writing–review and editing. **M. Dugo:** Data curation, formal analysis, writing–original draft. **D. Tosi:** Conceptualization, supervision, writing–review and editing. **C. Tacchetti:** Supervision. **T. Daniele:** Supervision, writing–review and editing. **B. Győrffy:** Data curation, supervision, writing–review and editing. **L. Sica:** Writing–review and editing. **M. Macchini:** Writing–review and editing. **M. Zambetti:** Writing–review and editing. **S. Zambelli:** Writing–review and editing. **G. Bianchini:** Conceptualization, supervision, funding acquisition, investigation, writing–original draft, writing–review and editing. **L. Gianni:** Conceptualization, data curation, supervision, funding acquisition, investigation, writing–original draft, writing–review and editing.

Acknowledgments

The study was supported in part by BCRF (grants no. 18-181 to L. Gianni and G. Bianchini), the Associazione Italiana per la Ricerca sul Cancro (AIRC; gramt no. IG 2018 - ID. 21787 project to G. Bianchini), and the Higher Education Institutional Excellence Programme (grant no. 2020–4.1.1.-TKP2020 to G. Bianchini) of the Ministry for Innovation and Technology in Hungary. This work has been also supported by an unrestricted grant of Pfizer Italia S.r.l. and Roche. We also thank Desiree Zambroni (Experimental Imaging Centre Ospedale San Raffaele, Milan, Italy)

for the assistance on the ImageStreamX use and Iommazzo Fabiola for technical assistance.

The publication costs of this article were defrayed in part by the payment of publication fees. Therefore, and solely to indicate this fact, this article is hereby marked "advertisement" in accordance with 18 USC section 1734.

Note

Supplementary data for this article are available at Clinical Cancer Research Online (http://clincancerres.aacrjournals.org/).

Received September 3, 2021; revised November 24, 2021; accepted March 3, 2022; published first March 7, 2022.

References

1. Prat A, Baselga J. The role of hormonal therapy in the management of hormonal-receptor-positive breast cancer with co-expression of HER2. Nat Clin Pract Oncol 2008;5:531–42.
2. Houston SJ, Plunkett TA, Barnes DM, Smith P, Rubens RD, Miles DW. Over-expression of c-erbB2 is an independent marker of resistance to endocrine therapy in advanced breast cancer. Br J Cancer 1999;79:1220–6.
3. Arpino G, Wiechmann L, Osborne C, Schiif R. Crosstalk between the estrogen receptor and the HER tyrosine kinase receptor family: molecular mechanism and clinical implications for endocrine therapy resistance. Endocr Rev 2008;29: 217–33.
4. Giuliano M, Hu H, Wang YC, Fu X, Nardone A, Herrera S, et al. Upregulation of ER signaling as an adaptive mechanism of cell survival in HER2-positive breast tumors treated with anti-HER2 therapy. Clin Cancer Res 2015;21:3995–4003.
5. Kaufman B, Mackey JR, Clemens MR, Bapsy PP, Vaid A, Wardley A, et al. Trastuzumab plus anastrozole versus anastrozole alone for the treatment of postmenopausal women with human epidermal growth factor receptor 2-positive, hormone receptor-positive metastatic breast cancer: results from the randomized phase III TAnDEM study. J Clin Oncol 2009;27:5529–37.
6. Johnston S, Pippen J Jr, Pivot X, Lichinitser M, Sadeghi S, Dieras V, et al. Lapatinib combined with letrozole versus letrozole and placebo as first-line therapy for postmenopausal hormone receptor-positive metastatic breast cancer. J Clin Oncol 2009;27:5538–46.
7. Lukas J, Bartkova J, Bartek J. Convergence of mitogenic signalling cascades from diverse classes of receptors at the cyclin D-cyclin-dependent kinase-pRb-controlled G1 checkpoint. Mol Cell Biol 1996;16:6917–25.
8. Prall OW, Rogan EM, Sutherland RL. Estrogen regulation of cell cycle progression in breast cancer cells. J Steroid Biochem Mol Biol 1998;65:169–74.
9. Yu Q, Geng Y, Sicinski P. Specific protection against breast cancers by cyclin D1 ablation. Nature 2001;411:1017–21.
10. Sherr CJ, Beach D, Shapiro GI. Targeting CDK4 and CDK6: From discovery to therapy. Cancer Discov 2016;6:353–67.
11. Finn RS, Dering J, Conklin D, Kalous O, Cohen DJ, Desai AJ, et al. PD 0332991, a selective cyclin D kinase 4/6 inhibitor, preferentially inhibits proliferation of luminal estrogen receptor-positive human breast cancer cell lines in vitro. Breast Cancer Res 2009;11:R77.
12. Agarwal R, Gonzalez-Angulo AM, Myhre S, Carey M, Lee JS, Overgaard J. et al. Integrative analysis of cyclin protein levels identifies cyclin b1 as a classifier and predictor of outcomes in breast cancer. Clin Cancer Res 2009;15:3654–62.
13. Finn RS, Crown JP, Lang I, Boer K, Bondarenko IM, Kulyk SO, et al. The cyclin-dependent kinase 4/6 inhibitor palbociclib in combination with letrozole versus letrozole alone as first-line treatment of oestrogen receptor-positive, HER2-negative, advanced breast cancer (PALOMA-1/TRIO-18): a randomised phase 2 study. Lancet Oncol 2015;16:25–35.
14. Cristofanilli M, Turner NC, Bondarenko I, Ro J, Im SA, Masuda N, et al. Fulvestrant plus palbociclib versus fulvestrant plus placebo for treatment of hormone-receptor-positive, HER2-negative metastatic breast cancer that progressed on previous endocrine therapy (PALOMA- 3): final analysis of the multicentre, double-blind, phase 3 randomised controlled trial. Lancet Oncol 2016;17:425–39.
15. Ma CX, Gao F, Luo J, Northfelt DW, Goetz M, Forero A, et al. NeoPalAna: neoadjuvant palbociclib, a cyclindependent kinase 4/6 inhibitor, and anastrozole for clinical stage 2 or 3 estrogen receptor–positive breast cancer. Clinical Cancer Res 2017;23:4055–65.
16. Sledge GW Jr, Toi M, Neven P, Sohn J, Inoue K, Pivot X, et al. MONARCH 2: abemaciclib in combination with fulvestrant in women with HR+/HER2-advanced breast cancer who had progressed while receiving endocrine therapy. J Clin Oncol 2017;35:2857–84.
17. Hortobagyi GN, Stemmer SM, Burris HA, Yap Y-S, Sonke GS, Paluch-Shimon S, et al. Ribociclib as first-line therapy for HR-positive, advanced breast cancer. N Engl J Med 2016;375:1738–48.
18. Turner NC, Slamon DJ, Ro J, Bondarenko I, Im SA, Masuda N, et al. Overall Survival with Palbociclib and Fulvestrant in Advanced Breast Cancer. N Engl J Med 2018;379:1926–36.
19. Goel S, Wang Q, Watt AC, Tolaney SM, Dillon DA, Li W, et al. Overcoming therapeutic resistance in HER2-positive breast cancers with CDK4/6 inhibitors. Cancer Cell 2016;29:255–69.
20. Gianni L, Bisagni G, Colleoni M, Del Mastro L, Zamagni C, Mansutti M, et al. Phase II neo-adjuvant treatment with trastuzumab and pertuzumab associated with palbociclib and fulvestrant in women with HER2-positive and ER-positive breast cancer - the NAPHER-2 Michelangelo study. Lancet Oncol 2018;19: 249–56.
21. Bliss CI. The calculation of microbal assays. Bacteriol Rev 1956;20:243–58.
22. Ianevski A, He L, Aittokallio T, Tang J. SynergyFinder: a web application for analyzing drug combination dose-response matrix data. Bioinformatics 2017;33: 2413–5.
23. Bianchini G, Iwamoto T, Qi Y, Coutant C, Shiang CY, Wang B, et al. Prognostic and therapeutic implications of distinct kinase expression patterns in different subtypes of breast cancer. Cancer Res 2010;70:8852–62.
24. Gorgoulis V, Adams PD, Alimonti A, Bennett DC, Bischof O, Bishop C., et al., et alet al. Cellular senescence: Defining a path forward. Cell 2019;179:813–27.
25. Foroutan M, Bhuva DD, Lyu R, Horan K, Cursons J, Davis MJ. Single sample scoring of molecular phenotypes. BMC Bioinf 2018;19:404.
26. Zhang K, et al. CDK4/6 inhibitor palbociclib enhances the effect of pyrotinib in HER2-positive breast cancer. Cancer Lett 2019;447:130–40.
27. Herrera-Abreu MT, Palafox M, Asghar U, Rivas MA, Cutts RJ, Garcia-Murillas I, et al. Early adaptation and acquired resistance to CDK4/6 inhibition in Estrogen receptor-positive breast cancer. Cancer Res 2016;76:2301–13.
28. Klein ME, Kovatcheva M, Davis LE, Tap WD, Koff A. CDK4/6 inhibitors: The mechanism of action may not be as simple as once thought. Cancer Cell 2018;34: 9–20.
29. Smith I, Robertson J, Kilburn L, Wilcox M, Evans A, Holcombe C, et al. Long-term outcome and prognostic value of Ki67 after perioperative endocrine therapy in postmenopausal women with hormone-sensitive early breast cancer (POETIC): an open-label, multicentre, parallel-group, randomised, phase 3 trial. Lancet Oncol 2020;21:1443–54.
30. Ellis MJ, Tao Y, Luo J, A'Hern R, Evans DB, Bhatnagar AS., et al. et alet al: Outcome prediction for estrogen receptor-positive breast cancer based on postneoadjuvant endocrine therapy tumor characteristics. J Natl Cancer Inst 2008;100:1380–8.
31. Liu Q, Yin X, Languino LR, Altieri DC. Evaluation of drug combination effect using a Bliss independence dose-response surface model. Stat Biopharm Res 2018;10:112–22.
32. Tosi D, Pérez-Gracia E, Atis S, Vié N, Combès E, Gabanou M, et al. Rational development of synergistic combinations of chemotherapy and molecular targeted agents for colorectal cancer treatment. BMC Cancer 2018;18:812.
33. Dulic V. Senescence regulation by mTOR. Methods Mol Biol 2013;965:15–35.
34. Im SA, Lu YS, Bardia A, Harbeck N, Colleoni M, Franke F, et al. Overall survival with ribociclib plus endocrine therapy in breast cancer. N Engl J Med 2019;25: 307–16.
35. Johnston SRD, Harbeck N, Hegg R, Toi M, Martin M, Shao ZM, et al. Abemaciclib combined with endocrine therapy for the adjuvant treatment of HR+, HER2-, node-positive, high-risk, early breast cancer (monarchE). J Clin Oncol 2020;1:3987–98.
36. Pancholi S, Ribas R, Simigdala N, Schuster E, Nikitorowicz-Buniak J, Ressa A, et al. Tumour kinome re-wiring governs resistance to palbociclib in oestrogen receptor positive breast cancers, highlighting new therapeutic modalities. Oncogene 2020;39:4781–97.
37. Mazumder A, Shiao S, Haricharan S. HER2 Activation and Endocrine Treatment Resistance in HER2-negative Breast Cancer. Endocrinology 2021;162:1–10.
38. Hutcheston IR, Goddard L, Barrow D, McClelland RA, Francies HE, Knowlden JM, et al. Fulvestrant-induced expression of ErbB3 and ErbB4 receptors

sensitizes oestrogen receptor-positive breast cancer cells to heregulin β1. Breast Cancer Res 2011;13:R29.
39. Wang YC, Morrison G, Gillihan R, Guo J, Ward RM, Fu X, et al. Different mechanisms for resistance to trastuzumab versus lapatinib in HER2-positive breast cancers—role of estrogen receptor and HER2 reactivation. Breast Cancer Res 2011;13:R121.
40. Frogne T, Benjaminsen RV, Sonne-Hansen K, Sorensen BS, Nexo E, Laenkholm AV, et al. Activation of ErbB3, EGFR and Erk is essential for growth of human breast cancer cell lines with acquired resistance to fulvestrant. Breast Cancer Res Treat 2009;114:263–75.
41. Punturi NB, Seker S, Devarakonda V, Mazumder A, Kalra R, Chen CH, et al. Mismatch repair deficiency predicts response to HER2 blockade in HER2-negative breast cancer. Nat Commun 2021;12:2940.
42. Sudhan DR, Schwarz LJ, Guerrero-Zotano A, Formisano L, Nixon MJ, Croessmann S, et al. Extended adjuvant therapy with neratinib plus fulvestrant blocks ER/HER2 crosstalk and maintains complete responses of ER+/HER2+ breast cancers: implications to the ExteNET trial. Clin Cancer Res 2019;25:771–83.
43. Sengupta S, Henry RW. Regulation of the retinoblastoma–E2F pathway by the ubiquitin–proteasome system. Biochim Biophys Acta 2015;1849:1289–97.
44. Ladd B, Mazzola AM, Bihani T, Lai Z, Bradford J, Michael C, et al. Effective combination therapies in preclinical endocrine resistant breast cancer models harboring ER mutations. Oncotarget 2016;7:54120–36.
45. Kovatcheva M, Liu DD, Dickson MA, Klein ME, O'Connor R, Wilder FO, et al. MDM2 turnover and expression of ATRX determine the choice between quiescence and senescence in response to CDK4 inhibition. Oncotarget 2015; 6:8226–43.
46. Stein GH, Drullinger LF, Soulard A, Dulić V. Differential roles for cyclin-dependent kinase inhibitors p21 and p16 in the mechanisms of senescence and differentiation in human fibroblasts. Mol Cell Biol 1999;19:2109–17.
47. Faget DV, Ren Q, Stewart SA. Unmasking senescence: context-dependent effects of SASP in cancer. Nat Rev Cancer 2019;19:439–53.
48. Nahta R, O'Regan RM. Therapeutic implications of estrogen receptor signaling in HER2-positive breast cancers. Breast Cancer Res Treat 2012;135:39–48.
49. Tolaney SM, Wardley AM, Zambelli S, Hilton J, Troso-Sandoval T, Ricci F, et al. MonarcHER: A randomized phase II study of abemaciclib plus trastuzumab with or without fulvestrant versus trastuzumab plus standard-of-care chemotherapy in women with HR+, HER2+ advanced breast cancer (ABC). Ann Oncol 2019; 30 Suppl 5:V861–2. Abstr nr LBA23.